Inorg. Chem. **2004**, *43*, 4127−4136

Quantum Mechanical Models of the Resting State of the Vanadium-Dependent Haloperoxidase

Giuseppe Zampella,[†,‡] Joslyn Yudenfreund Kravitz,[†,§] Charles Edwin Webster,[||] Piercarlo Fantucci,[‡] Michael B. Hall,[||] Heather A. Carlson,*[,§,⊥] Vincent L. Pecoraro,*[,§] and Luca De Gioia*[,‡]

Department of Biotechnology and Biosciences, University of Milano-Bicocca, Piazza della Scienza 2, 20126 Milano, Italy, Department of Chemistry, University of Michigan, Ann Arbor, Michigan 48109-1055, Department of Chemistry, Texas A&M University, College Station, Texas 77843, and Department of Medicinal Chemistry, College of Pharmacy, University of Michigan, Ann Arbor, Michigan 48109-1065

Received November 17, 2003

Density functional theory has been used to investigate structural and electronic properties of complexes related to the resting form of the active site of vanadium haloperoxidase as a function of environment and protonation state. Results obtained by studying models of varying size and complexity highlight the influence of environment and protonation state on the structure and stability of the metal cofactor. The study shows that, in the trigonal bipyramidal active site, where one axial position is occupied by a key histidine, the trans position cannot contain a terminal oxo group. Further, a highly negatively charged vanadate unit is not stable. Protonation of at least one equatorial oxo ligand appears necessary to stabilize the metal cofactor. The study also indicates that, while at rest within the protein, the vanadate unit is most likely an anion with an axial hydroxide and an equatorial plane containing two oxos and a hydroxide. For the neutral, protonated state of the vanadate unit, there were two minima found. The first structure is characterized by an axial water with two oxo and one hydroxo group in the equatorial plane. The second structure contains an axial hydroxo group and an equatorial plane composed of one oxo and two hydroxo oxygen atoms. These two species are not significantly different in energy, indicating that either form may be important during the catalytic cycle. These data support the initial crystallographic assignment of an axially bound hydroxide, but an axial water is also a possibility. This study also shows that the protonation state of the vanadate ion is most likely greater than previously proposed.

Introduction

Evidence of the involvement of vanadium ions in the vanadium-dependent haloperoxidase (VHPO)[1] enzymes has stimulated interest in biomimetic models for catalytic halogenation of organic substrates.[2] In general, haloperoxidases catalyze the two electron oxidation of halide ions via the following reaction scheme.[3]

$$H_2O_2 + H^+ + X^- \rightarrow H_2O + \text{“HOX”} \qquad (1)$$

The enzyme is named on the basis of its ability to oxidize a halide (X^-). Thus, chloroperoxidases can oxidize chloride, bromide, or iodide, whereas bromoperoxidases are incapable of using chloride as a substrate. The identity of “HOX” is dependent upon both the pH of the reaction and the halide involved. Initial studies indicated that the chloroperoxidase oxidizes a chloride ion to HOCl,[4] whereas the products of bromide oxidation are generally thought to be a thermodynamic distribution of Br_3^-, HOBr, and Br_2.[5] The “HOX”

* To whom correspondence should be addressed. E-mail: carlsonh@umich.edu (H.A.C.); luca.degioia@unimib.it (L.D.G.); vlpec@umich.edu (V.L.P).
† These authors contributed equally to this work.
‡ University of Milano-Bicocca.
§ Department of Chemistry, University of Michigan.
|| Texas A&M University.
⊥ Department of Medicinal Chemistry, College of Pharmacy, University of Michigan.

(1) Wever, R.; Kustin, K. In *Advances in Inorganic Chemistry*; Sykes, A. G., Ed.; Academic Press: New York, 1990; Vol. 35, pp 103−137.
(2) de la Rosa, R. I.; Clague, M. J.; Butler, A. *J. Am. Chem. Soc.* **1992**, *114*, 760−761.
(3) Everett, R. R.; Butler, A. *Inorg. Chem.* **1989**, *28*, 393−395.
(4) van Schijndel, J. W. P. M.; Barnett, P.; Roelse, J.; Vollenbroek, E. G. M.; Wever, R. *Eur. J. Biochem.* **1994**, *225*, 151−157.
(5) Butler, A. *Coord. Chem. Rev.* **1999**, *187*, 17−35.

10.1021/ic0353256 CCC: $27.50
Published on Web 04/16/2004

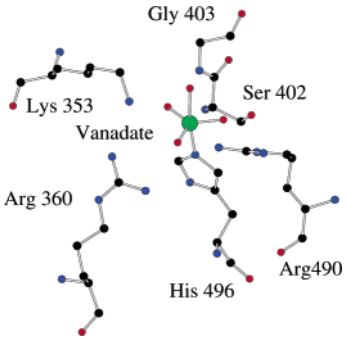

Figure 1. Atomic structure of the active site of the vanadium containing chloroperoxidase from the fungus *Curvularia inaequalis* as obtained from X-ray structure analysis.[7]

species can then halogenate an organic substrate if one is present. More recent work has suggested that certain organic substrates can be regioselectively halogenated,[6] presumably in the active site of the enzyme.

Of this enzyme family, the vanadium-dependent chloroperoxidase (VCPO) from the pathogenic fungus *Curvularia inaequalis* has been investigated the most thoroughly. Its X-ray crystal structure was the first of this family to be solved and has shed light on the characteristics of the active site of the enzyme.[7] Subsequent crystal structures of other VHPOs have revealed a drastic difference in the overall structure of the protein.[8,9] However, the entire first and second hydrogen-bonding shells for the cofactor are conserved across species, with the exception of the substitution of a histidine in the bromoperoxidase for a phenylalanine in the chloroperoxidase.[8] We will, therefore, refer to protein residues using the sequence and numbering in the 2.15 Å VCPO structure (PDB code 1VNI) of Messerschmidt and Wever.[7]

In the native state, the vanadate cofactor (VO_4^{3-}) is bound to the protein through a single covalent bond from the V to the N_ϵ of His496 (Figure 1). The high negative charge of the cofactor is offset by a number of protonated amino acids in the active site which donate hydrogen bonds to the oxygen atoms of the cofactor (Lys353, Arg360, His404, and Arg490). The crystal structure of this enzyme indicates that the vanadate unit is a trigonal bipyramidal structure with a hydroxide and His496 in the axial positions and three oxo moieties in the equatorial plane.[7]

There is no evidence that the vanadium undergoes redox cycling during catalysis, and hence, it is believed that the vanadium ion plays the role of a strong Lewis acid with respect to the primary oxidant, H_2O_2.[10] Kinetic studies suggest that protonation of the bound peroxo group is a crucial step in the heterolytic cleavage of the O−O bond. These proposals suggest that the protonated oxygen is then transferred to the halide according to an oxo-transfer mechanism.[11] Finally, the hypohalous acid formed can act as a stereoselective halogenating agent.[12]

Site-directed mutagenesis experiments (alanine scanning) have elucidated the relative importance of various active-site residues in catalytic activity.[13] His496 is the primary chemical anchor for vanadium, and its replacement with Ala results in complete loss of activity. Substitution of the positively charged residues Lys353, Arg360, and Arg490 revealed less severe effects, but of these mutants, the largest decrease in activity is observed for K353A. In fact, Lys353 is the only residue which interacts with the peroxo-bound moiety directly. It has been suggested that it plays a role in polarizing the peroxo bond, making it more susceptible to nucleophilic attack.[14] The crystal structures indicate that Arg490 is involved in two hydrogen bonds with oxygen atoms of the cofactor, both in the native and the peroxo forms, whereas Arg360 donates only one hydrogen bond. This difference in participation is reflected in the milder reduction of catalytic efficiency shown by the R360A mutant with respect to K353A and R490A.

Peroxo−vanadium complexes are good functional models of the VHPO and have been shown to epoxidize alkenes,[15] hydroxylate hydrocarbons,[16] and oxidize many organic[17] and inorganic compounds,[18] including alcohols[19] and sulfides.[20] However, attempts to synthesize structural models of the VHPO active site have not been as successful, and a synthetic complex reproducing the exact coordination environment of vanadium in VHPO has not yet been obtained. It has been proposed that such a complex has not been isolated because a five-coordinate imidazole complex is unstable unless sequestered in a protein active site.[21] Therefore, synthetic models have thus far provided limited insight into structural and electronic features of the vanadium cofactor. In this context, quantum mechanics calculations are useful tools to investigate structural and electronic properties of models of the active site of metalloenzymes. Though computational investigations of vanadium complexes have been reported,[22,23] the ligand sets of the complexes in previous studies did not reflect the coordination environment of the

(6) Martinez, J. S.; Carrol, G. L.; Tschirret-Guth, R. A.; Altenhoff, G.; Little, R. D.; Butler, A. *J. Am. Chem. Soc.* **2001**, *123*, 3289−3294.
(7) Messerschmidt, A.; Wever, R. *Proc. Natl. Acad. Sci., U.S.A.* **1996**, *93*, 392−396.
(8) Weyand, M.; Hecht, H.-J.; Kie, M.; Liaud, M.-F.; Vilter, H.; Schomburg, D. *J. Mol. Biol.* **1999**, *293*, 595−611.
(9) Isupov, M. N.; Dalby, A. R.; Brindley, A. A.; Izumi, Y.; Tanabe, T.; Murshudov, G. N.; Littlechild, J. A. *J. Mol. Biol.* **2000**, *299*, 1035−1049.
(10) de Boer, E.; Boon, K.; Wever, R. *Biochemistry* **1988**, *27*, 1629−1635.
(11) Colpas, G. J.; Hamstra, B. J.; Kampf, J. W.; Pecoraro, V. L. *J. Am. Chem. Soc.* **1996**, *118*, 3469−3478.
(12) Clague, M. J.; Keder, N. L.; Butler, A. *Inorg. Chem.* **1993**, *32*, 4754−4761.
(13) Hemrika, W.; Renirie, R.; Macedo-Ribeiro, S.; Messerschmidt, A.; Wever, R. *J. Biol. Chem.* **1999**, *274*, 23820−23827.
(14) Messerschmidt, A.; Prade, L.; Wever, R. *Biol. Chem.* **1997**, *378*, 309−315.
(15) Sheldon, R. A.; Kochi, J. K. *Metal-catalyzed oxidations of organic compounds: mechanistic principles and synthetic methodology including biochemical processes*; Academic Press: New York, 1981.
(16) Mimoun, H.; Saussine, L.; Daire, E.; Postel, M.; Fischer, J.; Weiss, R. *J. Am. Chem. Soc.* **1983**, *105*, 3101−3110.
(17) Conte, V.; DiFuria, F.; Moro, S. *J. Phys. Org. Chem.* **1996**, *9*, 329−336.
(18) Butler, A.; Clague, M. J.; Meister, G. E. *Chem. Rev.* **1994**, *94*, 625−638.
(19) Bartolini, O.; Conte, V.; Di Furia, F.; Modena, G. *Nouv. J. Chim.* **1985**, *9*, 147−150.
(20) Smith, T. S., II; Pecoraro, V. L. *Inorg. Chem.* **2002**, *41*, 6754−6760.
(21) Ligtenbarg, A. G. J. In *Chemistry*; University of Groningen: Groningen, Holland, 2001.
(22) Buhl, M. *J. Comput. Chem.* **1999**, *20*, 1254−1261.
(23) Conte, V.; Bortolini, O.; Carraro, S.; Moro, S. *J. Inorg. Biochem.* **2000**, *80*, 41−49.

vanadium atom observed in the enzyme. In this paper, we report results obtained using density functional theory (DFT) to investigate structural properties of complexes related to the native form of VCPO as a function of environment and protonation state.

Computational Methods

All calculations presented in this paper were performed using Gaussian 98.[24] Quantum chemical calculations were carried out using models of four sizes, based on the first shell of residues in contact with the vanadate cofactor. Bond distances and angles for all models were taken from the crystal structure of the enzyme.[7] The smallest models used an ammonia in place of His496 and contained no external hydrogen-bonding molecules. The second set of models was expanded to include contributions from one hydrogen-bonding partner in the active site, represented by ammonia or ammonium, depending on the charge state desired. The third set of models was expanded once again, and small molecule models which more closely resembled the active-site residues were included. His496 was modeled with an imidazole, and Lys353 and Arg490 were modeled by methylamine and guanidine, respectively. Guanidinium and ammonium can be considered acceptable structural models for the polar heads of arginine and lysine, respectively, but they are expected to be slightly less basic than the corresponding amino acids.[25] Finally, the largest scaffolds were expanded to include the six amino acids from the crystal structure that appear to be donating hydrogen bonds to the cofactor. In addition to Arg490, another guanidinium and a glycyl-serine dipeptide were added to represent Arg360, Ser402, and Gly403, respectively. The representative group for Lys353 was reduced to an ammonium cation, and the representative group for His496 was changed to be a methylimidazole molecule. Additionally, a crystallographically derived water was included to act as a hydrogen-bonding partner for the axial oxygen ligand. Due to the size of the scaffolds (61−62 atoms), a lower level of theory was required.

With the exception of the largest models, all calculations were carried out using DFT.[26] They employed the hybrid exchange-correlation functional, B3LYP.[27] The basis set used for vanadium was the effective core potential basis set of Hay and Wadt (LanL2DZ)[28] as modified by Couty and Hall (341/341/41 for V), where the two outermost p functions have been replaced by a (41) split of the optimized 4p function.[29] The cc-pVDZ[30] basis set was used for N and O atoms, and D95[31] for hydrogens. Full geometry optimizations were carried out, and minima were verified through frequency calculations.

Scheme 1. Schematic Representation of the Starting Structures Used in Calculations To Investigate Native Models of the Active Site of VCPO[a]

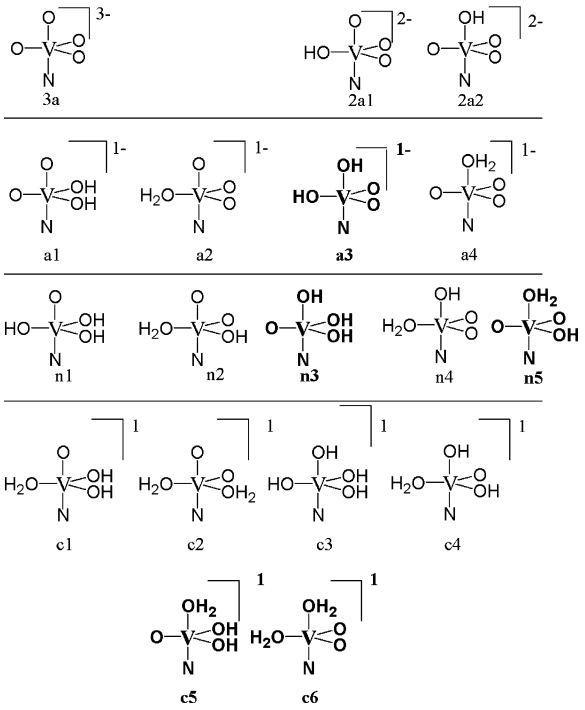

[a] N is either an ammonia molecule or an imidazole. Complexes which minimize to biologically relevant structures are shown in bold.

The largest models underwent a series of partial optimizations at the Hartree−Fock level of theory and using LanL2DZ for V and D95V[31] for all other atoms. All hydrogens were minimized as well as the vanadate oxygens and the imidazole ring in the axial position. Vanadium and the heavy atoms of the protein and water were held fixed.

Figures were drawn using ChemEdit.[32]

Results

In Scheme 1, the figures, and tables, the models used in this study have been labeled with an alphanumeric designation defined as follows: The first part of the name refers to the charge state of the vanadate cluster (a, n, or c, to designate anionic, neutral, or cationic structures, respectively). A preceding number indicates the charge of the system if it is not one or zero (i.e., 3a for the −3 charge state). The letter is followed by a number which corresponds to the starting structure of the vanadate unit as defined in Scheme 1. For complexes with one or more external hydrogen-bonding molecules (Figures 3−5), the vanadate structure code will be followed by a superscript for each external molecule. The superscript will be either K, n, or c representing a potassium ion, a neutral hydrogen-bond donor, or positively charged hydrogen-bonding molecule, respectively. For species with

(24) Frisch, M. J.; Trucks, G. W.; Schlegel, H. B.; Scuseria, G. E.; Robb, M. A.; Cheeseman, J. R.; Zakrzewski, V. G.; Montgomery, J. A., Jr.; Stratmann, R. E.; Burant, J. C.; Dapprich, S.; Millam, J. M.; Daniels, A. D.; Kudin, K. N.; Strain, M. C.; Farkas, O.; Tomasi, J.; Barone, V.; Cossi, M.; Cammi, R.; Mennucci, B.; Pomelli, C.; Adamo, C.; Clifford, S.; Ochterski, J.; Petersson, G. A.; Ayala, P. Y.; Cui, Q.; Morokuma, K.; Malick, D. K.; Rabuck, A. D.; Raghavachari, K.; Foresman, J. B.; Cioslowski, J.; Ortiz, J. V.; Stefanov, B. B.; Liu, G.; Liashenko, A.; Piskorz, P.; Komaromi, I.; Gomperts, R.; Martin, R. L.; Fox, D. J.; Keith, T.; Al-Laham, M. A.; Peng, C. Y.; Nanayakkara, A.; Gonzalez, C.; Challacombe, M.; Gill, P. M. W.; Johnson, B. G.; Chen, W.; Wong, M. W.; Andres, J. L.; Head-Gordon, M.; Replogle, E. S.; Pople, J. A. *Gaussian 98*, revision A.11.1; Gaussian, Inc.: Pittsburgh, PA, 1998.
(25) Tantillo, D. J.; Chen, J.; Houk, K. N. *Curr. Opin. Chem. Biol.* **1998**, *2*, 743−750.
(26) Parr, R. G.; Yang, W. *Density-Functional Theory of Atoms and Molecules*; Oxford University Press: Oxford, U.K., 1989.
(27) Lee, C.; Yang, W.; Parr, R. G. *Phys. Rev. B* **1988**, *37*, 785−789.
(28) Hay, P. J.; Wadt, W. R. *J. Chem. Phys.* **1985**, *83*, 270−283.
(29) Couty, M.; Hall, M. B. *J. Comput. Chem.* **1996**, *17*, 1359−1370.
(30) Woon, D.; Dunning, T. H. J. *J. Chem. Phys.* **1993**, *98*, 1358−1371.
(31) Dunning, T. H. J.; Hay, P. J. In *Modern Theoretical Chemistry*; Schaefer, H. F., III, Ed.; Plenum: New York, 1976; Vol. 3, pp 1−28.
(32) Lim, C. E.; Jorgensen, W. L. In *Encyclopedia of Computational Chemistry*; Schleyer, P. v. R., Ed.; John Wiley and Sons: New York, 1998; Vol. 5, p 3295.

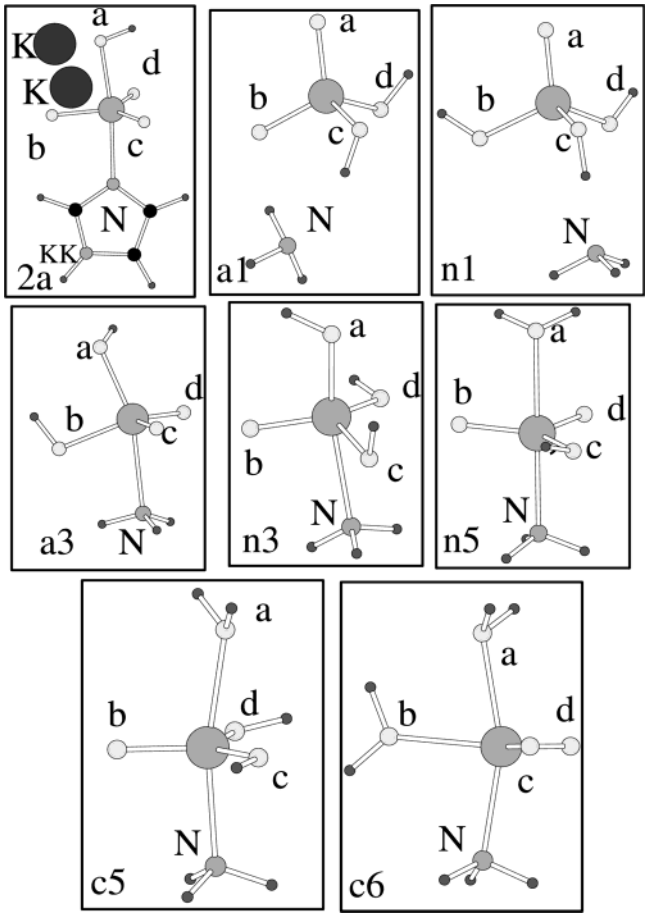

Figure 2. Calculated minima of non-hydrogen-bonded structures. Atom labels correspond to those in Table 1. Panel $\mathbf{2a^{KK}}$ shows the minimized structure of the dianionic vanadate unit with two potassium atoms included in the calculation. Panels **a1** and **n1** show the structures of the global minima for the anionic and neutral units, respectively. Panels **a3**, **n3**, and **n5** show the biologically relevant minima for their respective charge states. Panels **c5** and **c6** show the low energy cationic structures.

more than one local energy minimum, the alphanumeric designation will also contain the subscript i, ii, iii, or iv, depending on the number of minima observed. The bound amine ligand, which mimics His496, will be referred to generically as N. The identity of N (imidazole or ammonia) will be specified as appropriate.

No External Hydrogen-Bonding Group (Figure 2). (VO_4^{-3})N and (HVO_4^{-2})N (Scheme 1: 3a, 2a1, and 2a2). Initially, we investigated the structural properties of models of the active site without the stabilizing influence of the protein environment. Optimization of unprotonated (**3a**) and singly protonated (**2a1** and **2a2**) structures led to separation of each into a tetrahedral vanadate and an amine. The results were the same when either imidazole or ammonia occupied the axial N position. The calculation was repeated for the imidazole complexes using an extended basis set (triple-ζ + polarization on all atoms) and two different functionals (B3LYP and BP86[33]). Similar results were obtained for all methods (data not shown).

To investigate whether neutralizing the negative charge of the complex would improve its stability, two K^+ ions were

(33) Becke, A. D. *Phys. Rev. A* **1988**, *38*, 3098−3100. Perdew, J. P. *Phys. Rev. B* **1986**, *33*, 8822−8824; **1986**, *34*, 7406.

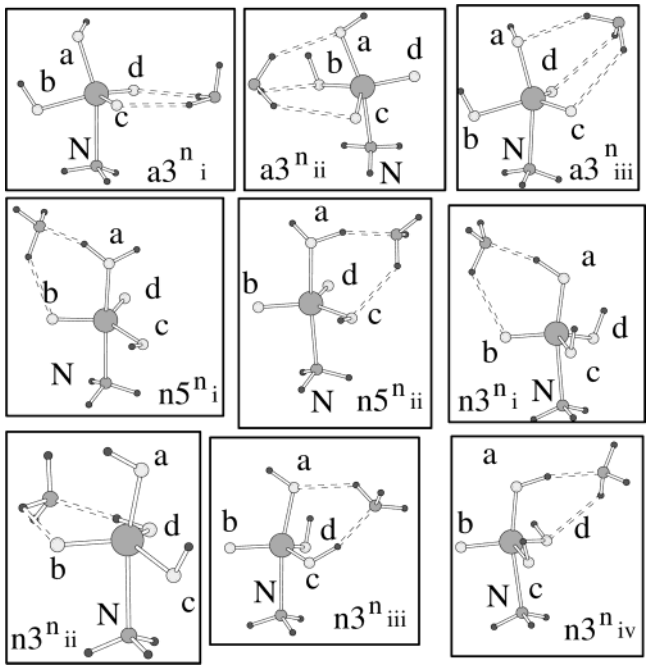

Figure 3. Calculated minima of anionic and neutral structures with one added hydrogen-bonding molecule. Atom labels correspond to those in Table 2. The panels in the top row show the anionic minima in order of increasing energy from left to right. The first two panels of the second row show the minimum structures for a neutral vanadate unit with an axial water. The last panel in the second row shows the minimum structure for a neutral vanadate unit with an axial hydroxo moiety. The panels of the third row show other low-energy structures of this type with energy increasing from left to right.

added to the HVO_4^{2-}−imidazole model (Figure 2, $\mathbf{2a^{KK}}$). In the optimized complex, the N−V bond was not cleaved, but it was significantly longer (2.216 Å) than that reported in the X-ray structure of the enzyme (1.96 Å).[14]

$H_2VO_4NH_3^{-1}$ and $H_3VO_4NH_3$ (Scheme 1: a1−4 and n1−5). In order to efficiently examine all possible anionic and neutral species, a minimal model was used. There were four possible monoanionic complexes with the formula $H_2VO_4NH_3^{-1}$ and five possible neutral complexes with the formula $H_3VO_4NH_3$ (Scheme 1, **a1**−**4** and **n1**−**5**). In both charge states, the lowest-energy structure was a tetrahedral vanadate with a dissociated ammonia (Figure 2, **a1** and **n1**). None of the structures with an oxo group axial to the ammonia resulted in stable five-coordinate structures (Scheme 1, **a1**, **a2**, **n1**, and **n2**). The lowest-energy, five-coordinate species in each charge state had a hydroxo group in the axial position (Figure 2, **a3** and **n3**). A neutral species with water in the axial position was also a stable minimum (Figure 2, **n5**) but was 3.2 kcal/mol higher in energy than the axial hydroxo structure. Important bond distances and angles for these complexes are shown in Table 1. The final structures for **a2**, **a4**, **n2**, and **n4** are neither biologically relevant nor low in energy so they are not shown (their structures are available in the Supporting Information).

$H_4VO_4NH_3^{+1}$ (Scheme 1: c1−6). There were six cationic isomers of the model, all of which remained five-coordinate upon minimization (Scheme 1, **c1**−**6**). However, only half maintained the trigonal bipyramidal arrangement with the ammonia in one of the axial positions. The lowest-energy

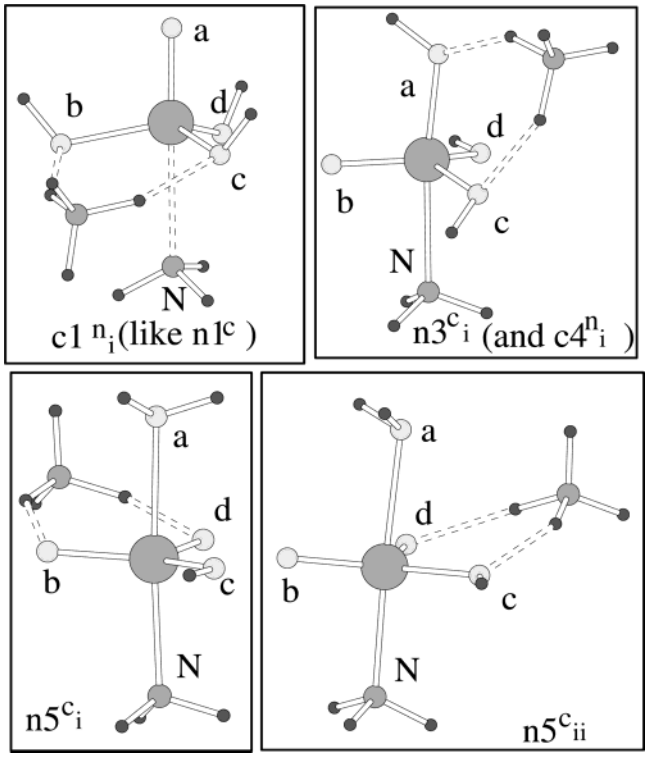

Figure 4. Calculated minima of cationic structures with one added hydrogen-bonding molecule. Atom labels correspond to those in Table 3. Panel **c1$^{n}_{i}$ /n1^{c}** shows a high-energy minimum with an axial oxo group. Panels **n3$^{c}_{i}$** and **n5$^{c}_{i}$** show the two minimum structures of the overall cationic species, which are almost equal in energy. Panel **n5$^{c}_{ii}$** shows a higher energy minimum which is an isomer of **n5$^{c}_{i}$**.

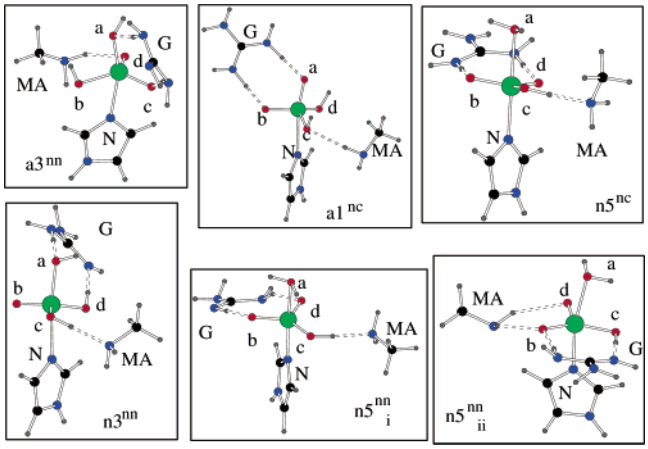

Figure 5. Calculated minima of structures with two added hydrogen-bonding molecules. Atom labels correspond to those in Table 4. G stands for guanidine, and MA stands for methylamine. Panel **a3^{nn}** shows the minimum structure for an overall anionic species. Panel **a1^{nc}** shows the minimum structure for an overall neutral species containing an anionic vanadate unit and a protonated guanidinium molecule. Panel **n5^{nc}** shows the minimum structure of a cationic species containing a neutral vanadate unit and a protonated guanidinium molecule. The panels in the bottom row show three nearly energetically equivalent overall neutral structures.

cation (Figure 2, **c5**) had water and ammonia in the axial positions, and an oxo and two hydroxos in the equatorial plane. The second lowest-energy cation (Figure 2, **c6**) contained two waters, one of which was trans to the ammonia, and two oxos in the equatorial plane. Of the remaining four cations (**c1**−**4**, structures available in Supporting Information), the highest-energy structure had four hydroxo groups (**c3**), and although it remained trigonal bipyramidal, it was extremely high in energy (over 18 kcal/mol higher than **c5**) and is not considered to be biologically relevant. In **c1**, **c2**, and **c4**, the vanadate rearranged so that there was no longer a clear axis made up of one oxo ligand and the amine. The bonding parameters and relative energies of **c5** and **c6** are in Table 1.

One External Hydrogen-Bonding Molecule (Figures 3 and 4). $H_2VO_4NH_3^{-1}$ + NH_3 and $H_3VO_4NH_3$ + NH_3 (Scheme 1: a1−**4 and n1**−**5).** External hydrogen-bonding molecules were added to the models. In the anionic case, addition of an ammonia molecule to each unique position in the equatorial plane did not significantly change the behavior or structure of the molecules. Loss of the bound ammonia to yield a tetrahedral vanadate again led to the lowest-energy structure (**a1^{n}**, not shown). Addition of a hydrogen-bond donor to **a3** led to three five-coordinate structures, all within 1 kcal/mol, which differed only in the position of ammonia with respect to the equatorial ligands (Figure 3, **a3$^{n}_{i-iii}$**). The various **a2** and **a4** models rearranged to four-coordinate vanadium species which were much higher in energy than the five-coordinate minima (structures not shown). The bond angles and distances for the vanadate unit in structures **a1^{n}** and **a3$^{n}_{i-iii}$** are virtually the same as those for **a1** and **a3**, respectively (Table 1), so only the hydrogen-bond interactions and relative energies for **a1^{n}** and **a3$^{n}_{i-iii}$** are listed in Table 2.

In the case of the neutral species, 20 starting structures were minimized (two for **n1**, six for **n2**, and four each for **n3**−**5**, each with the additional ammonia molecule hydrogen bonding to each distinct oxygen ligand in both the axial and equatorial positions). The only biologically relevant structures were found to be the same as in the previous section (Figure 3, **n3$^{n}_{i-iv}$** and **n5$^{n}_{i-ii}$**). The lowest-energy structures, **n5$^{n}_{i}$** and **n3$^{n}_{i}$**, had an axial ligand donating a hydrogen bond to the free ammonia, but several other five-coordinate conformers were found to be stable minima. For the axial water case, the other minimum had the free ammonia donating a hydrogen bond to the equatorial hydroxide, rather than the oxo (**n5$^{n}_{ii}$**). This configuration was within 1 kcal/mol in energy of **n5$^{n}_{i}$**. In the axial hydroxide case, there were three minima (**n3$^{n}_{ii-iv}$**) approximately 3 kcal/mol higher in energy than **n3$^{n}_{i}$**. These four structures have roughly the same geometry about the vanadium but differ in the identities of the donors and acceptors of the hydrogen bonds (Figure 3). The majority of the bond angles and distances for structures **n3$^{n}_{i-v}$** and **n5$^{n}_{i-ii}$** are virtually the same as those in Table 1, so only hydrogen-bond interactions and relative energies are given in Table 2.

Like the anionic case, the vanadium would not remain five-coordinate with an oxo group trans to the bound ammonia. However, the lowest-energy, neutral species was five-coordinate, unlike the anionic case.

$H_3VO_4NH_3$ + NH_4^+ and $H_4VO_4NH_3^+$ + NH_3 (Scheme 1: n1−**5 and c1**−**6).** The hydrogen bonds for overall cationic species were modeled as (1) a neutral vanadate complex with an external ammonium ion and (2) a cationic vanadate complex with an external ammonia molecule. The

Table 1. Bonding Parameters for Important Non-Hydrogen-Bonding Vanadate Species

name[a]	V−Oa[b]	V−Ob[b]	V−Oc[b]	V−Od[b]	V−N[b]	Ob−V−Oa[c]	Ob−V−N[c]	Ob−V−Oc[c]	Ob−V−Od[c]	Oa−V−N[c]	ΔE[d]
2a^{KK}	2.11	1.71	1.67	1.67	2.26	85.7	87.1	118.0	118.3	172.8	N/A
a1	1.63	1.65	1.82	1.85	3.53	113.3	55.3	108.0	108.2	146.9	0
a3	1.88	1.92	1.64	1.64	2.29	88.8	72.6	119.1	121.2	161.2	+13.6
n1	1.59	1.79	1.74	1.79	3.71	110.7	85.9	109.5	108.1	151.6	0
n3	1.81	1.59	1.83	1.80	2.26	102.4	88.5	117.6	112.5	165.4	+5.14
n5	2.22	1.62	1.82	1.62	2.14	86.3	94.6	125.1	114.4	−179.8	+8.34
c5	2.11	1.57	1.76	1.76	2.12	98.8	93.4	114.3	110.9	167.8	0
c6	2.12	2.12	1.59	1.59	2.12	75.2	85.7	125.1	125.1	160.9	+6.37

[a] Complexes as defined in Scheme 1. [b] Distances in Å. [c] Angles in deg. [d] Difference in energy, in kcal/mol, as compared to lowest-energy structure of a given charge state.

Table 2. Hydrogen-Bonding Interactions in Structures as in Figure 3

structure	O···H−N distance[a]	O···H−N angle[b]	N···H−O_{eq} distance[a]	N···H−O_{eq} angle[b]	O_{ax}···H···N distance[a]	O_{ax}···H···N angle[b]	ΔE[c]
a1^{n}	1.95	160.1	2.02	153.1			0
a3$^{n}_{i}$	2.22 (to d)	144.3					12.05
	2.23 (to c)	143.7					
a3$^{n}_{ii}$	2.36 (to b)	139.5			2.35 (to a)	134.9	12.28
	2.56 (to c)	127.6					
a3$^{n}_{iii}$	2.52 (to c)	127.2			2.27 (to a)	145.1	12.90
	2.73 (to d)	126.1					
n5$^{n}_{i}$	2.08 (to b)	136.9			1.65 (from a)	162.6	0
n5$^{n}_{ii}$	2.15 (to c)	137.1			1.66 (from a)	158.5	0.979
n3$^{n}_{i}$	2.28 (to b)	127.9			1.68 (from a)	164.5	0.786
n3$^{n}_{ii}$	2.61 (to b)	124.5	1.74 (to d)	165.5			2.40
n3$^{n}_{iii}$			1.72 (to c)	161.3	2.19 (to a)	137.0	2.72
n3$^{n}_{iv}$	2.30 (to d)	135.5			1.77 (from a)	159.4	3.53

[a] Distances in Å. [b] Angles in deg. [c] Difference in energy, in kcal/mol, as compared to lowest-energy structure of a given charge state.

Table 3. Hydrogen-Bonding Interactions in Cationic Structures as in Figure 4

structure	O···H−N distance[a]	O···H−N angle[b]	O_{ax}···H−N distance[a]	O_{ax}···H−N angle[b]	ΔE[c] vs n3$^{c}_{i}$
c1$^{n}_{i}$ (n1^{c})	1.79 (to b)	149.8			+5.37
	1.79 (to c)	150.0			
n3$^{c}_{i}$	1.79 (to c)	144.3	1.64	149.3	0
n5$^{c}_{i}$	1.88 (to b)	140.8			+0.320
	1.73 (to d)	150.1			
n5$^{c}_{ii}$	1.79 (to c)	147.0	N/A	N/A	+4.19
	1.82 (to d)	148.9			

[a] Distances in Å. [b] Angles in deg. [c] Energy difference in kcal/mol.

Table 4. Hydrogen-Bonding Interactions in Structures with Abbreviations as In Figure 5

	G−H···O distance[a]	G−H···O angle[b]	G···H−O distance[a]	G···H−O angle[b]	MA···H···O distance[a]	MA···H···O angle[b]
n3^{nn}	1.82 (to a)	117.6	1.71 (to d)	176.4	1.80 (from c)	170.2
n5$^{nn}_{i}$	2.21 (to b)	178.9			1.81 (from c)	175.5
	2.00 (to d)	154.2				
n5$^{nn}_{ii}$	1.93 (to b)	174.1	1.75 (to c)	177.1	2.36 (to b)	135.9
					2.34 (to b)	137.7
n5^{nc}	1.71 (to b)	177.4			1.68 (from c)	176.8
	1.73 (to d)	178.8				
a3^{nn}	1.88 (to a)	173.1			2.11 (to d)	158.5
	1.90 (to c)	167.8				
a1^{nc}	1.58 (to a)	179.2			2.12 (to c)	169.7
	1.54 (to b)	178.6				

[a] Distances in Å [b] Angles in deg.

external molecules were placed in all unique positions in the equatorial plane to create a series of minima in both states. After minimization, it was found that the type 1 structures were significantly lower in energy than the type 2 complexes. In fact, some type 2 starting structures transferred a proton from the vanadate unit to the ammonia resulting in type 1 minima. Specifically, one such complex started as a **c5^{n}** structure and minimized to a structure similar to **n3^{c}** (this structure is not shown in Figure 4 because it was too high in energy to be considered biologically relevant, but both the starting and minimum coordinates are available in the Supporting Information).

The type 1 structures yielded several five-coordinate minima that were similar to the overall neutral minima (Figure 4, **n3$^{c}_{i}$** and **n5$^{c}_{i−ii}$**). However, these biologically relevant structures were not the global minima. The lowest-energy, biologically relevant structure had a hydroxo in the axial position (Figure 4, **n3$^{c}_{i}$**), and the structure with a water trans to the ammonia (Figure 4, **n5$^{c}_{i}$**) was very close in energy. Related structures were significantly higher in energy (Figure 4, **n5$^{c}_{ii}$** and **n3$^{c}_{ii}$**, not shown).

Of the type 2 species, only two were biologically relevant (**c5^{n}** and **c6^{n}**, structures not shown). These two complexes were both over 10 kcal/mol higher in energy than the lowest-energy, type 1 species, and the additional ammonia molecule accepted a hydrogen bond from the bound ammonia rather than donating hydrogen bonds to the oxygen ligands. Hydrogen-bonding parameters for low-energy, biologically relevant overall cationic structures are in Table 3. The starting and minimized coordinates, as well as the final energies for all structures, can be found in the Supporting Information.

Two External Hydrogen-Bonding Molecules (Figure 5). External molecules that were more representative of the protein active site were incorporated: N was an imidazole molecule and Lys353 and Arg490 were modeled in their crystallographic positions by methylamine and guanidine, respectively.

Table 5. Bonding Parameters for **a3**^{ncc} and **a3**^{nnc} [a]

	V−X distance[c]	Ob−V−X angle[d]	H-bond 1 distance[c]	H-bond 1 angle[d]	H-bond 2 distance[c]	H-bond 2 angle[d]	H-bond 3 distance[c]	H-bond 3 angle[d]
				a3^{ncc}				
Oax	1.87	84.0	2.55	160.8				
Ob	1.84		1.67 (K353)	168.2	2.01 (G403)	164.7		
Oc	1.62	114.1	1.77 (R360)	164.4	2.10 (R490)	175.4		
Od	1.60	136.5	1.82 (S402)	168.0	2.00 (R490)	172.8		
N[b]	2.15	88.8						
				a3^{nnc}				
Oax	1.90	87.8	2.25	173.2				
Ob	1.81		1.83 (K353)	169.0	1.91 (to R360)	163.3		
Oc	1.64	126.6	2.45 (R360)	165.3	1.75 (R490)	150.3	2.00 (R490)	141.1
Od	1.58	121.9	1.62 (S402)	176.2	2.09 (G403)	118.3		
N[b]	2.12	82.8						

[a] Oax and Ob are hydroxo groups. Oc and Od are oxo groups. Oax accepts a hydrogen bond from water. [b] Oa−V−N angle = 171.2° for **a3**^{ncc} and 166.6° for **a3**^{nnc}. [c] Distances in Å. [d] Angles in deg.

HVO_4N^{2-} + Externals (Scheme 1, 2a1−2). Minimization of the HVO_4^{2-}−imidazole adduct resulted in V−N bond cleavage (structures available in Supporting Information).

$H_2VO_4N^{1-}$ + Externals and H_3VO_4N + Externals, (Scheme 1: a3, n1, n3, and n5). There was one stable, five-coordinate, anionic species (Figure 5, **a3**^{nn}). In this complex, the guanidine became involved in hydrogen bonds with the axial hydroxo and one equatorial oxo groups. Hydrogen-bonding parameters are listed in Table 4. Calculations with either a protonated methylamine or guanidine resulted in proton transfer to an oxo group. To verify that this result was not an artifact of the higher acidity of methylamine and guanidine with respect to lysine and arginine, models which included the full amino acid side chains were also optimized, and proton transfer to the oxo groups was observed (data not shown).

Protonation of **a3**^{nn} resulted in three neutral vanadate isomers (Figure 5, **n3**^{nn}, **n5**$^{nn}_{i}$, and **n5**$^{nn}_{ii}$). The stabilities of these species were similar, with energy differences on the order of a few kcal/mol. One anionic vanadate species with a cationic guanidinium group, yielding an overall neutral structure (Figure 5, **a1**^{nc}) was also investigated. In this case, it was again observed that the imidazole did not completely dissociate, but it remained at a weakly bonding distance (2.47 Å). Only one stable, overall monocationic species was found (Figure 5, **n5**^{nc}). The neutral vanadate group was composed of an axial water, one hydroxo, and two oxo groups. The cationic guanidine did not protonate the vanadate during minimization. Hydrogen-bonding interactions are listed in Table 4.

Hydrogen-Bonding Scaffold (Figure 6). Calculations of the largest, most biologically relevant scaffold showed that a vanadate unit carrying a highly negative charge (−3 or −2) was not stable and lost the imidazole. In the case of a dianionic vanadate (**2a2**^{ccc} and **2a2**^{ncc}, structure not shown), allowing the protons to minimize while all the heavy atoms were held fixed resulted in one proton from the ammonia being almost immediately transferred to an equatorial oxo group. This transfer generated the two structures, both with an anionic vanadate unit, that were used in the remaining calculations: an overall neutral structure in which one guanidine was deprotonated (Figure 6, **a3**^{nnc}), and an overall cation in which both guanidinium molecules were protonated (Figure 6, **a3**^{ncc}).

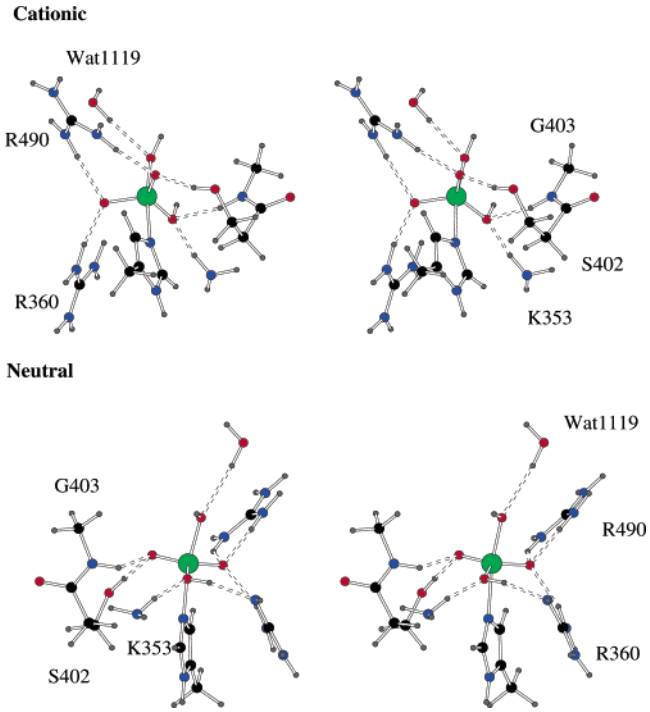

Figure 6. Stereoview of calculated partial minima of anionic vanadate units contained in overall cationic (**a3**^{ncc}) and overall neutral (**a3**^{nnc}) representative hydrogen-bonding scaffolds.

In both final structures, the axial hydroxo accepted a hydrogen bond from the nearby crystallographic water, and each equatorial ligand accepted two hydrogen bonds from the scaffold. In the overall cationic structure (**a3**^{ncc}), the equatorial oxygens minimized to positions that closely resembled the crystal structure (average displacement was only 0.29 Å). In the overall neutral structure (**a3**^{nnc}), the equatorial ligands moved on average 0.93 Å from their crystallographic positions, rotating approximately 34° within the equatorial plane to allow the equatorial hydroxide to donate a hydrogen bond to the deprotonated guanidine. This resulted in one additional hydrogen bond between the cofactor and the scaffold. Bonding parameters for these models are listed in Table 5.

Discussion

Although the vanadium-dependent haloperoxidases comprise a rather rare family of enzymes, their ability to stereoselectively halogenate natural organic molecules makes them very important.[6] These compounds are often the leads for new pharmaceuticals or precursors to polymeric materials. A better fundamental understanding of how these enzymes work, and more specifically, what role the vanadate cofactor plays in the catalytic cycle, will be immensely beneficial to both the natural products and inorganic chemistry communities. The DFT calculations of the haloperoxidase presented in this paper allow us to look more closely at this elusive metal center and make suggestions as to its role in the catalytic process. Although the coordinates for the starting structures in this study are taken from the crystal structure of the chloroperoxidase,[7] the results can be extended to the entire enzyme family since only residues which are conserved in all haloperoxidases[8,9] were used in the models.

It has been suggested that the structure of all VHPO active sites is dianionic and trigonal bipyramidal. It purportedly contains three oxo groups in the equatorial plane and one hydroxo ligand trans to His496, which provides the only covalent bond to the protein (Figure 1).[14] However, the resolution of the highest quality crystal structure currently available is 2.0 Å, and the protons are not visible,[8] so the exact ligand set and protonation state of the cofactor are not strictly known. Therefore, in our studies we explored all permutations of oxo, hydroxo, and water groups as ligands for the vanadium in various charge states (Scheme 1). In order to make this complete search tractable, we used the smallest system possible: $H_xVO_4NH_3^y$, where $0 \leq x \leq 4$ and $-3 \leq y \leq 1$. The arrangement proposed in the crystal structure is $x = 1$, $y = -2$.

Minimization of a tri- or dianionic vanadate unit resulted in dissociation of the ammonia and a tetrahedral vanadate (Scheme 1, **3a1** and **2a1**−**2**). Replacing the ammonia with imidazole did not stabilize the structure. The addition of one, two, or seven hydrogen-bonding groups in the vicinity of the complex was also insufficient to stabilize the complex. However, addition of two potassium ions to the HVO_4^{2-} system resulted in a stable, overall neutral complex (Figure 2, $\mathbf{2a^{KK}}$). These results highlight the importance of buffering the negative charge on the cofactor, supporting previous proposals suggesting this role for the protein residues forming the active site.[13]

Upon minimization of the four anionic, five neutral, and six cationic structures shown in Scheme 1, we found that under no circumstances was a structure with a terminal oxo trans to the ammonia stable (Figure 2). The weakening of the bond to the ammonia is most likely a result of the sizable electron donation from the axial oxo to the vanadium (the strong trans influence of the oxo). In all anionic and neutral cases initiated with that arrangement (**a1**−**2** and **n1**−**2**), one neutral ligand (water or ammonia) dissociated from the complex and donated a hydrogen bond back to the tetrahedral vanadate. While not biologically relevant, structures **a1** and **n1** are the global minima for their respective charge states. In the cationic cases, the ligands rearranged, without dissociation, to nonbiologically important geometries (**c1**−**2**). It would seem that dissociation of a neutral ligand to leave a cationic vanadium species is less favorable. Only in the cationic case is the biologically relevant, trigonal bipyramidal species the lowest-energy structure (Figure 2, **c5**). In the anionic and neutral cases, the lowest-energy, biologically relevant structures have hydroxide in the trans position (Figure 2, **a3** and **n3**), which supports the proposed axial hydroxo group from the crystal structure study. It should be noted, however, that this is dependent upon the ligands in the equatorial plane. The presence of three equatorial oxo ligands, as proposed in the crystal structure, leads to decomposition of the vanadate unit. There is also a stable neutral complex with an axial water (Figure 2, **n5**) which is 3.2 kcal/mol higher in energy than **n3**, but there is no stable anion with water in any position.

In order to determine if any of the unstable structures could be stabilized by hydrogen bonds, we introduced an external ammonia molecule to each structure in various positions. In the anionic case, there was no significant change. The tetrahedral conformations were always the global minima for the anions. In the neutral case, the vanadate did not remain five-coordinate with a terminal oxo group trans to the bound ammonia. However, the interaction with the external ammonia did make the five-coordinate structure with an axial water the global minimum for the neutral species (Figure 3, $\mathbf{n5_i}$). There were five such low-energy complexes that maintained the trigonal bipyramidal geometry upon minimization ($\mathbf{n5_{i-ii}}$ and $\mathbf{n3_{i-iii}}$).

For investigation of cationic systems, two types of structures were used: a cationic vanadate unit with hydrogen bonds to an ammonia molecule and a neutral vanadate unit with hydrogen bonds to an ammonium cation. The overall cationic system was more stable if the vanadium unit was neutral than if the vanadium unit carried the positive charge. The two lowest-energy structures, which were almost energetically identical, both contained neutral vanadate (Figure 4, $\mathbf{n3^c_i}$ and $\mathbf{n5^c_i}$). Interestingly, the difference in energy between the two neutral vanadate minima decreases as the complexity of the system is increased. The observed trend is the following: **n3** is more than 3 kcal/mol lower in energy than **n5**; $\mathbf{n5^n_i}$ is 0.8 kcal/mol lower in energy than $\mathbf{n3^n_i}$, but $\mathbf{n3^c_i}$ is only 0.3 kcal/mol lower in energy than $\mathbf{n5^c_i}$.

On the basis of the above results, we wanted to determine the effects of multiple hydrogen-bond donors that simultaneously complement several of the oxygen ligands on vanadium. This led us to investigate our next level of models which incorporated an environment that was more representative of the protein active site. In place of two ammonia molecules, we used an imidazole, a methylamine, and a guanidine to mimic His496, Lys353, and Arg490, respectively. Under all previous conditions there were a limited number of stable configurations of the vanadate cofactor. It was not feasible to study all possibilities in the large system, so we based the conformations of the large systems on the stable smaller models (Figure 5).

Results obtained investigating this model indicate that hydrogen bonds between methylamine or guanidine and an HVO_4^{2-} cofactor (Scheme 1) were not sufficient to withdraw enough electron density from the metal center to stabilize the five-coordinate complex. Remarkably, optimization of any dianionic vanadium complex initially complemented by charged hydrogen-bonding groups resulted in proton transfer to an oxo group to give a monoanionic vanadate structure (Figure 5, **a3**$^{\mathbf{nn}}$). This was similar to the anions minimized with only one added ammonia. In fact, if structures **a3**$^{\mathbf{n}}_{\mathbf{i}}$ and **a3**$^{\mathbf{n}}_{\mathbf{ii}}$ are overlaid, the resultant three hydrogen bonds are the same as those seen in **a3**$^{\mathbf{nn}}$.

In the neutral case, we do not see quite the same correspondence between models. In the large model, neither **n5**$^{\mathbf{nn}}_{\mathbf{i}}$ nor **n5**$^{\mathbf{nn}}_{\mathbf{ii}}$, shown in Figure 5, has any hydrogen bond to the axial water, while that is the only hydrogen-bonding interaction in **n5**$^{\mathbf{n}}_{\mathbf{i}}$ and **n5**$^{\mathbf{n}}_{\mathbf{ii}}$. Further, in **n3**$^{\mathbf{nn}}$ (Figure 5), the axial hydroxo group is positioned over the equatorial hydroxos and accepts a hydrogen bond, but in the smaller model (Figure 3, **n3**$^{\mathbf{n}}$), the axial hydroxo is rotated so that it is above the equatorial oxo and is donating a hydrogen bond. We also calculated the minimum structures and their energies for models with one external ammonia molecule that more closely resembled the large one. These calculations included models where the axial hydroxo either accepted or donated a hydrogen bond, but both cases were significantly higher in energy than the original models (data given in Supporting Information).

Comparison of structures in Figure 5 to the depiction of the crystal structure in Figure 1[5] shows that in **n3**$^{\mathbf{nn}}$ there was a large shift in the position of the guanidine to make the axial hydrogen bond. This shift did not occur in the **n5**$^{\mathbf{nn}}$ cases. A similar rearrangement of R490 is observed in the H404A mutant form of the protein,[34] suggesting that this large movement is connected to the lack of the imidazole ring interacting with the axially bound hydroxide. This shift probably occurred in **n3**$^{\mathbf{nn}}$ in order to make the axial position more waterlike, which was not necessary for **n5**$^{\mathbf{nn}}$.

The above behavior would seem to indicate that an axial water is preferred over an axial hydroxide, which agrees with results obtained using smaller models. Careful examination of Figure 4 shows that the axial hydroxo in **n3**$^{\mathbf{c}}_{\mathbf{i}}$ accepts a very tight hydrogen bond from the external ammonium (2.61 Å), making that ligand quite waterlike and almost identical in energy to **n5**$^{\mathbf{c}}_{\mathbf{i}}$ (in which the ammonium did not interact with the axial water at all). Conversely, **n5**$^{\mathbf{n}}_{\mathbf{i}}$ was 0.8 kcal/mol lower in energy than **n3**$^{\mathbf{n}}_{\mathbf{i}}$ whose axial hydroxo was not waterlike at all.

We have also investigated one anionic vanadate species with a cationic guanidinium, yielding an overall neutral structure. This complex (Figure 5, **a1**$^{\mathbf{nc}}$) was related to the anionic structure that rearranged to be tetrahedral in previous cases (Figure 2, **a1**). Hence, we again saw that the imidazole was lost, but like **n1**$^{\mathbf{n}}_{\mathbf{ii}}$, the amine remained trans to the oxo but at a nonbonding distance. Remarkably, **a1**$^{\mathbf{nc}}$ was less stable than **n3**$^{\mathbf{nn}}$ by only 0.66 kcal/mol.

(34) Macedo-Ribeiro, S.; Hemrika, W.; Renirie, R.; Wever, R.; Messerschmidt, A. *J. Biol. Inorg. Chem.* **1999**, *4*, 545−559.

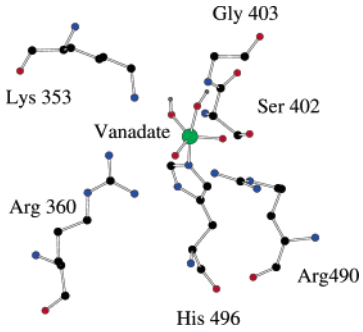

Figure 7. Structure of active site, as in Figure 1, with proposed resting protonation state.

A stable minimum which contained a protonated guanidinium was found for one overall monocationic species (Figure 5, **n5**$^{\mathbf{nc}}$) where its proton was not transferred to the neutral metal cofactor. This is in agreement with the smaller models where protonation of the external hydrogen-bonding group led to lower-energy complexes than the corresponding cationic vanadate units. The structure of **n5**$^{\mathbf{nc}}$ resembled **n5**$^{\mathbf{nn}}_{\mathbf{i}}$, differing by longer V−O bond distances and shorter hydrogen bonds due to the strong Coulombic interaction of the oxo groups with the positively charged guanidinium residue. As in **n5**$^{\mathbf{nn}}_{\mathbf{i}}$, we did not see a hydrogen bond to the axial water in **n5**$^{\mathbf{n}}$.

The partial optimization of the largest scaffolds (Figure 6) resulted in very similar structures that are consistent with the smaller models. Even with the plethora of hydrogen bonds available to the vanadate, neither a highly charged unit nor an axial oxo was stable. Additionally, the axial hydroxo accepted a hydrogen bond from the nearby crystallographic water in both cases. The main difference between the two structures is that minimizing the overall neutral structure (Figure 6, **a3**$^{\mathbf{nnc}}$) resulted in a significant rotation of the oxygens within the equatorial plane which allowed the hydroxide to donate a hydrogen bond to the neutral guanidine. The six hydrogen bonds from the scaffold were redistributed among the cofactor ligands so that none of the interactions were lost. Thus, the net number of hydrogen bonds for the equatorial oxygens was seven, rather than six as seen in the crystal and overall cationic scaffold (Figure 6, **a3**$^{\mathbf{ncc}}$) structures. Since the minimized, cationic scaffold most closely resembles the crystal structure, it is likely that the active site is fully protonated.

The discussion above may shed some light on to the resting state of the VCPO. These studies indicate that the vanadate cofactor is most likely anionic with several charges from the environment complementing the cofactor and creating a net neutral or cationic state for the active site. If the vanadate cofactor were neutral in the resting state, it would probably oscillate between the **n3** and **n5** type structures. Calculations indicate that addition of a proton to either state would likely result in protonation of a side chain rather than the cofactor. Further, these calculations suggest three things about the anionic cofactor. First, the axial position is not occupied by a terminal oxo. Second, in a stable state, there is most likely a hydroxo trans to His496 and another hydroxo in the equatorial plane (Figure 7) as in **a3**.

Last, the ideal position at which this cofactor is protonated would seem to be dependent upon the kinetics of the reaction. Protonation at the equatorial hydroxo would lead to an **n4** type structure which is unstable and would lose the water molecule quite quickly forming a high-energy, four-coordinate vanadate. This would be the preferred protonation site if peroxide were already in the active site when the reaction begins. However, protonation at either the axial position or at an equatorial oxo yields **n3** or **n5** species, respectively, which appear close enough in energy in the protein that they probably interconvert. This species could be stable long enough for a peroxide molecule to enter the active site and displace the water to begin the catalytic cycle. In fact, protonation of the axially coordinated hydroxide group in the native state of the enzyme (**n5**$^{\mathbf{nn}}_{\mathbf{i-ii}}$ and **n5**$^{\mathbf{nc}}$) has been proposed to be a crucial step of the VCPO catalytic cycle.[35]

Conclusion

The goal of this study was to further our understanding of the early intermediates of the vanadium dependent chloroperoxidase catalytic cycle. On the basis of crystallographic data, we generated computational models of the active-site vanadate unit with increasing contributions from the surrounding protein scaffold. Investigation of various charge states and ligand arrangements suggest that an anionic vanadate cofactor, consisting of an axial hydroxo group with a hydroxo group and two oxo moieties in the equatorial plane, is most stable when complemented by the hydrogen bonds of the protein active site in its resting state. The initial protonation of the catalytic cycle may occur at the axial hydroxo or an equatorial oxo leading to reasonable intermediate structures of varying reactivity.

Acknowledgment. The authors wish to thank the following funding agencies for support of this work: NIH GM42703 (V.L.P.), NIH GM65372 (H.A.C.), Beckman Young Investigator Program (H.A.C.), NIH GM008270 Michigan Molecular Biophysics Training Grant (J.Y.K.), NSF CHE 98-00184 (M.B.H.), and the Welch Foundation, Grant A-648 (M.B.H.).

Supporting Information Available: Starting and final coordinates, as well as final energies, for all minimized complexes. Sample input file and figure showing the minimized structures for the nonbiologically relevant structures. This material is available free of charge via the Internet at http://pubs.acs.org.

IC0353256

(35) Hamstra, B. J.; Colpas, G. J.; Pecoraro, V. L. *Inorg. Chem.* **1998**, *37*, 949−955.